THE KLOE DETECTOR: STATUS REPORT AND FIRST RESULTS

The KLOE collaboration: M. Adinolfi, A. Aloisio, F. Ambrosino, A. Andryakov, A. Antonelli, M. Antonelli, F. Anulli, C. Bacci, A. Bankamp, G. Barbiellini, G. Bencivenni, S. Bertolucci, C. Bini, C. Bloise, V. Bocci, F. Bossi, P. Branchini, S.A. Bulychjov, G. Cabibbo, A. Calcaterra, R. Caloi, P. Campana, G. Capon, G. Carboni, A. Cardini, M. Casarsa, G. Cataldi, F. Ceradini, F. Cervelli, F. Cevenini, G. Chiefari, P. Ciambrone, S. Conetti, S. Conticelli, E. De Lucia, G. De Robertis, R. De Sangro, P. De Simone, G. De Zorzi, S. Dell'Agnello, A. Denig, A. Di Domenico, C. Di Donato, S. Di Falco, A. Doria, E. Drago, O. Erriquez, A. Farilla, G. Felici, A. Ferrari, M. L. Ferrer, G. Finocchiaro, C. Forti, A. Franceschi, P. Franzini, M. L. Gao, C. Gatti, P. Gauzzi, S. Giovannella, V. Golovatyuk, E. Gorini, F. Grancagnolo, W. Grandegger, E. Graziani, P. Guarnaccia, U.v. Hagel, H.G. Han, S.W. Han, X. Huang, M. Incagli, L. Ingrosso, Y. Y. Jiang, W. Kim, W. Kluge, V. Kulikov, F. Lacava, G. Lanfranchi, J. Lee-Franzini, T. Lomtadze, C. Luisi, C. S. Mao, M. Martemianov, M. Matsyuk, W. Mei, L. Merola, R. Messi, S. Miscetti, A. Moalem, S. Moccia, M. Moulson, S. Mueller, F. Murtas, M. Napolitano, A. Nedosekin, M. Panareo, L. Pacciani, P. Pagès, M. Palutan, L. Paoluzi, E. Pasqualucci, L. Passalacqua, M. Passaseo, A. Passeri, V. Patera, E. Petrolo, G. Petrucci, D. Picca, G. Pirozzi, C. Pistillo, M. Pollack, L. Pontecorvo, M. Primavera, F. Ruggieri, P. Santangelo, E. Santovetti, G. Saracino, R. D. Schamberger, C. Schwick, B. Sciascia, A. Sciubba, F. Scuri, I. Sfiligoi, J. Shan, P. Silano, T. Spadaro, S. Spagnolo, E. Spiriti, C. Stanescu, G.L. Tong, L. Tortora, E. Valente, P. Valente, B. Valeriani, G. Venanzoni, S. Veneziano, Y. Wu, Y.G. Xie, P.P. Zhao, Y. Zhou.

The paper describes the KLOE detector which has been operating at the Frascati φ factory DAΦNE since the beginning of 1999. The performances of the different detector components are presented together with the calibration techniques used. A data sample of about 2.4 pb^{-1} was collected during the first physics run in Nov-Dec 1999. Preliminary results on radiative φ decays obtained from the analysis of this sample are also presented.

1 Introduction

KLOE [1] was mainly designed to study direct CP violation in neutral kaon decays, aiming at an accuracy of 10^{-4} on the measurement of $\Re(\varepsilon'/\varepsilon)$. The detector is operational at the Frascati φ factory DAΦNE since the beginning of 1999. DAΦNE [2] is a double annular e^+ e^- collider working at the φ resonance $\sqrt{s}$=1020 MeV, the design luminosity being 5×10^{32} $\mathrm{cm}^{-2}\mathrm{s}^{-1}$. The relevant decay channel for direct CP violation studies is $\varphi \longrightarrow K^0 \bar{K^0}$, with a branching ratio of 34.3% [3]. Kaons are produced almost back to back and have an average momentum of $\sim$ 110 MeV/c. An additional distinctive property of this decay is the fact that C invariance forces the two neutral kaons to be in a well defined $K_S K_L$ quantum state: this allows us to efficiently tag the presence of a K_L (K_S) by means of identifying the decay products of the corresponding K_S(K_L) in the opposite detector's hemisphere; it also allows us to perform quantum interferometry studies for a first determination of $\Im(\varepsilon'/\varepsilon)$ and for a precise determination of $\Re(\varepsilon'/\varepsilon)$. KLOE will also employ the standard double ratio technique used by fixed target experiments [4] to determine $\Re(\varepsilon'/\varepsilon)$: an accurate control of systematic effect and of the detector response is of the greatest importance to achieve the desired precision. The detector [5] consists of, in order of increasing radius, a cylindrical drift chamber, a hermetic electromagnetic calorimeter and a solenoidal superconducting coil, providing a 0.6 T field (Fig 1). The calibration methods used

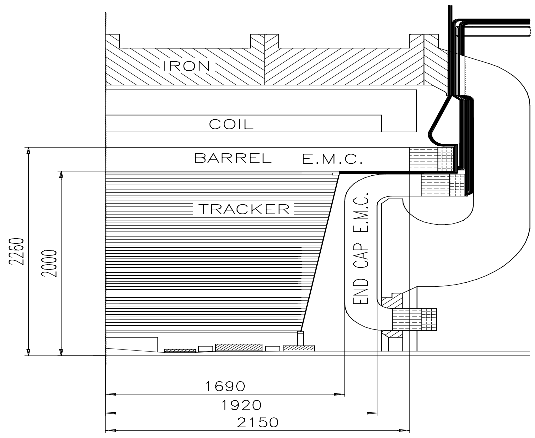

Figure 1: Cross section of $\frac{1}{4}$ of the KLOE detector.

and the perfomance of the different subdetectors are presented in the following paragraphs. The KLOE physic program is not restricted to the issue of direct CP violation: radiative φ decays can be studied already in the first period of DAΦNE operation, allowing for example the measurement of the η η' mixing angle and the clarification of the nature of the a_0 and f_0's. Preliminary results on same radiative φ decays are also presented in this paper.

2 The drift chamber (DC)

The KLOE drift chamber has been designed to optimize detection and reconstruction of the $K_L \longrightarrow \pi^+\pi^-$ decays, aiming at the precise determination of the decay vertex: the required accuracy on the vertex position is $\sim$ 1 mm [6]. The mean decay path for a K_L in KLOE is $\sim$ 3.4 m, therefore the decay vertices populate a large volume. The momentum spectrum of the decay products is essentially flat between 150 and 270 MeV/c. The chamber dimensions, the drift cells shape, the magnetic field value and the gas mixture chosen are determined by the above considerations. The need for a very large fiducial volume leads to a cylindrical chamber with a radius of $\sim$ 2 m and a length of $\sim$ 3.3 m. The isotropy of the decay product leads us to a full stereo geometry of the drift cells which ensure the highest uniformity in filling the sensitive volume. Multiple scattering and photon conversions in the chamber walls are kept under control by employing low Z material (carbon fiber) for the chamber structure and low mass Helium based gas mixture (90% He 10% i-C_4H_{10}, X_0=900 (gas+wires)). The $\sim$ 12600 cells of the chamber are organized in 58 circular layers. In order to improve the resolution on the determination of the K_S decay vertex and the K_S direction, the outer 46 layers consist of 3×3 cm^2 cells, while the inner 12 layers consists of smaller 2×2 cm^2 cells. Consecutive layers have stereo angles of opposite sign and increasing with radius from a lower value of ∼ 60 mrad to ∼ 150 mrad. Due to the peculiar cell geometry and to the drift properties of the Helium based gas mixture the calibration of the space to time relation (R-T) is done using 232 different R-T relations. The calibration is accomplished using cosmics rays that assure a uniform illumination for all the different R-T relations. The chamber calibration is an iterative procedure in which the tracks are reconstructed using an approximated R-T relation which is iteratively improved until the mean value of the tracks residuals is well below 50 μm. As a by-product of this procedure, the cell resolution is found to be less than 150 μm over almost all the drift distance, well below the design resolution value of 200 μm . After chamber calibration, K_S and K_L charged decays were studied. K_S charged decays are selected requiring two oppositely charged tracks forming a vertex in the K_S fiducial region, a 5 cm radius sphere centered on the interaction point. The invariant mass of the two tracks is required to be compatible with the K_S mass within a very loose cut of about 200 MeV /c^2 (assuming the mass of the pion for both tracks) while the total K_S momentum is required to be within 50 and 170 MeV/c . The mass resolution is about 1 MeV/c^2 as shown in (Fig 2 A), in good agreement with the one expected from the drift chamber resolution and with the KLOE design value.

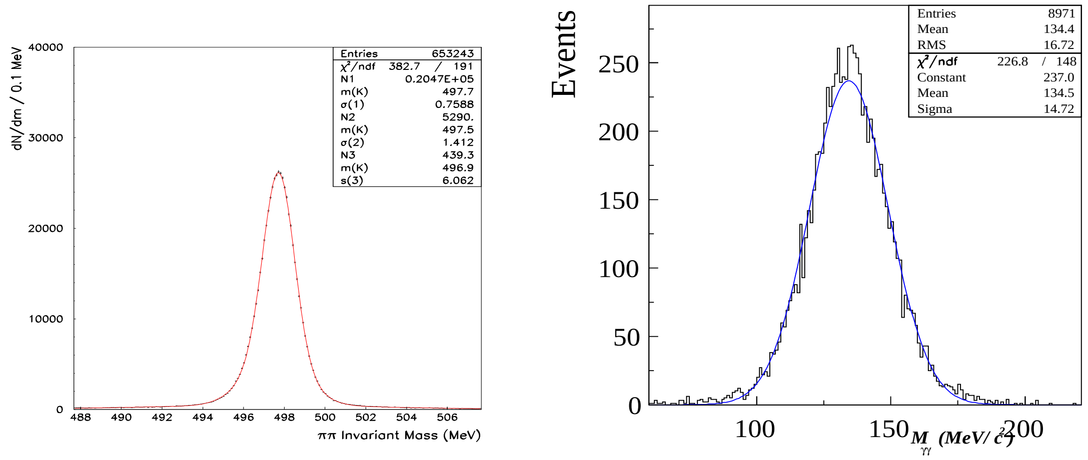

Figure 2: A) Reconstructed K_S mass in $K_S \longrightarrow \pi^+\pi^-$. B) Reconstructed π^0 mass in $\varphi \to \pi^+\pi^-\pi^0$ events.

3 The electromagnetic calorimeter (EMC)

The EMC [5] main tasks are to measure the $K_{S,L}$ neutral vertex with ∼ 1 cm accuracy, to discriminate $K_L \to 2\pi^0$ from $K_L \to 3\pi^0$ decays, and to provide a fast, unbiased first level trigger. The calorimeter is organized as a barrel part and two end-cap sections plus two small scintillating tiles calorimeters (QCAL) that instrument the low β quadrupoles. The barrel consists of 24 lead-scintillating fibers straight modules, while each end-cap is formed by 32 lead-scintillating fibers C shaped modules: each module is segmented in depth in 5 samplings and is divided in columns (∼ 4 × 4 cm^2), the total number of read out photomultipliers is 4880. The fiber:lead:glue volume ratio is 50:40:10, with an energy sampling fraction of 13%. The high ratio of scintillating fibers and lead results in a very good detection efficiency, even for photon energies as low as 20 MeV. The fast scintillating fibers used (Kuraray and Poli.hi.tech) assure the excellent time resolution needed to reconstruct the K_L neutral vertex position with ∼ 1 cm accuracy. The calorimeter energy calibration is performed using cosmic rays to equalize the cells response, a feature needed for triggering, plus Bhabha and $\gamma\gamma$ events to set the absolute energy scale. The linearity and the resolution as a function of energy is measured using radiative Bhabha events in which the e^+ and e^- momenta are measured with the drift chamber. The linearity is better than 1 % over the full energy range (20-500 MeV) and the resolution can be parametrized as σ(E)/E $\sim$ 5.7%/$\sqrt{E(GeV)}$ + 0.006. The absolute energy calibration is checked by reconstructing the two-photon invariant mass for $\varphi \to \pi^+\pi^-\pi^0$ events. This gives a π^0 mass of 133 MeV/c^2 (σ = 16 MeV/c^2) which is uniform across the whole EMC, to better than 1% (Fig 2 B).

The time calibration of the calorimeter is achieved by equalizing all the cells using cosmic rays. The absolute time scale is set using $\gamma\gamma$ events, which are generated in the interaction point: from the measured impact position on the calorimeter it is possible to estimate the photon flight path and then calculate the absolute time of the measured energy clusters. The measured times are then rescaled to this absolute time. The same technique is also used to associate each event with its machine crossing time (the DAΦNE bunch crossing time is 2.7 ns and the trigger is asynchrounous with it). The time resolution as a function of energy is measured using radiative Bhabha events and the result can be parametrized as : σ(t)$\sim$ 54 psec/$\sqrt{E/(GeV)} \oplus 147ps$.

This time resolution translates in a a neutral vertex resolution, measured with $K_L \longrightarrow \pi^+\pi^-\pi^0$ events, of about 1.6 cm, which is very close to the KLOE design value.

4 Radiative φ decays

The first physics data taking for KLOE took place in Nov-Dec 1999. The collected data sample is 2.4 pb^{-1} corresponding to about 7.7$\times$10^6 recorded φ decays. This sample has been analysed to study both the detector performance as discussed in the previous sections and some of the most relevant radiative φ decays. Preliminary results on the measurements of the branching ratios for $\varphi \longrightarrow \eta\gamma$, $\varphi \longrightarrow \eta'\gamma$, $\varphi \longrightarrow f_0\gamma$ are presented in the following.

4.1 $\varphi \longrightarrow \eta\gamma$, $\eta \longrightarrow \gamma\gamma$

This decay has a very clear signature given by the presence of three prompt photons with energies in the range 150 $< E_\gamma <$ 500 MeV. The radiative γ has an energy of about 360 MeV and an angular distribution described by $(1 + cos^2\theta)$ where θ is the polar angle. The main background comes from the $\varphi \longrightarrow \pi^0\gamma$ decay and it is effectively reduced cutting on the energy of the photons coming from the η decay, $|\Delta E| = |E_1 - E_2| <$ 300 MeV. A kinematic fit is performed on the obtained event sample and the final distributions for the ΔE, polar angle and energy of the radiative γ and the η mass for the 18500$\pm$140 selected events, corresponding to 1.84 pb^{-1}, are shown in Fig 3.

Experimental data and MonteCarlo simulation of the decay are in good agreement. KLOE preliminary result on the $\varphi \longrightarrow \eta\gamma$ branching ratio as related to the $\varphi \longrightarrow \pi^0\gamma$ branching ratio is: $B(\varphi \to \eta\gamma)/B(\varphi \to \pi^0\gamma)$ = 3.75 $\pm$ 0.08 (stat) $\pm$ 0.24 (syst), to be compared with the PDG '98 value of 3.78 $\pm$ 0.40. The preliminary systematic error is dominated by the presently incomplete knowledge of the triggering and filtering efficiency.

4.2 $\varphi \longrightarrow \eta'\gamma$

Measuring the $\varphi \to \eta'\gamma$ branching ratio is relevant both for the study of the η' gluonic content and for the determination of the η_8, η_1 mixing angle between the octect-singlet pseudoscalar states that mix to produce the physical η and η' states. The value of $B(\varphi \to \eta\gamma)/B(\varphi \to \eta'\gamma)$ can be related to the octect-singlet η_8, η_1 mixing angle; a measurement with a 10% accuracy of this ratio would lead to an error of about 1^0 on the mixing angle. Large gluonic contents in the η' would reflect in a very small branching ratio of $\sim 10^{-6}$ for this radiative φ decay. The

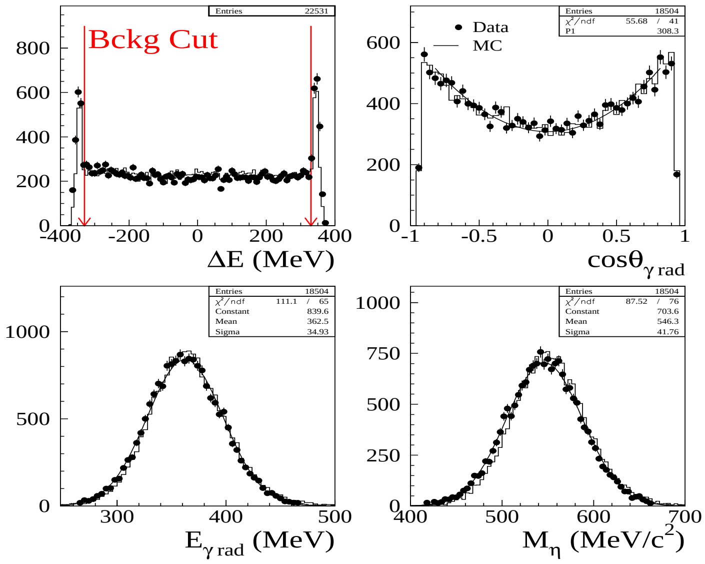

Figure 3: $\varphi \to \eta\gamma$ decays. a) $|\Delta E|$ distribution, b) radiative photon polar angle distribution, c) radiative photon energy distribution, d) reconstructed η mass. Experimental data (dots) and Montecarlo prediction (solid histogram) are shown.

measurement of this branching ratio has been performed using both charged and fully neutral η' decays. The charged decay chain under study is $\varphi \longrightarrow \eta'\gamma$, $\eta' \longrightarrow \eta\pi^+\pi^-$, $\eta \longrightarrow \gamma\gamma$. Event selection requires a vertex with two charged tracks close to the φ origin, and three prompt γ's at polar angles larger than 21^0 to reduce spurious clusters. Assuming the π mass for the two charged tracks, their total energy should be less than 412 MeV while the total energy of the photon clusters is required to be larger than 520 MeV. After performing this cuts the only remaining background is the $\varphi \longrightarrow \eta\gamma$ decay. This is effectively reduced by a kinematic fit and by a cut on the χ^2 probability for an event to be signal or background: $\mathrm{P}(\chi^2_{\eta'\gamma}) > 25$ % AND $P(\chi^2_{\eta\gamma}) < 1\%$. The efficiency of this selection is about 23%, leading to a final signal to noise ratio larger than 35 (90% confidence level). We remain with a total of 21 selected events (see Fig. 4) from which we measure: $B(\varphi \to \eta\gamma)/B(\varphi \to \eta'\gamma) = (7.1 \pm 1.6 \pm 0.3) \times 10^{-3}$.

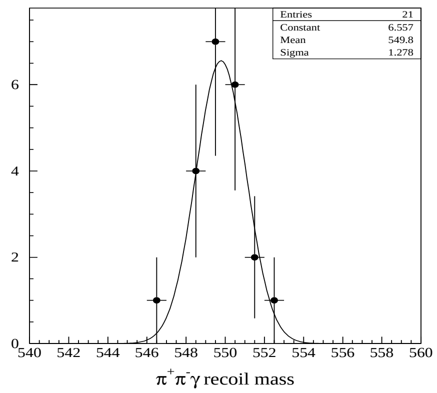

Figure 4: The missing mass in the $\pi^+\pi^-\gamma$ selected events, this quantity peak at the η mass.

The fully neutral decay chain $\varphi \longrightarrow \eta'\gamma$, $\eta' \longrightarrow \eta\pi^0\pi^0$, $\eta \longrightarrow \gamma\gamma$, would result in a 7 γ's final state. This signal events are selected requiring the presence of 7 prompt γ's at an angle $> 21^0$ having a total energy compatible with the φ mass (within 2 σ_E=130 MeV). Moreover the energy of the most energetic photon must be greater than 300 MeV. The efficiency of those cuts is about 47 %. A kinematic fit on the selected events is performed and further cuts to discriminate between the signal and the $\eta\gamma \longrightarrow 7\gamma$ background are applied. The total efficiency of the selection cuts is 12.6 % with a signal to background ratio larger than 13. We made the first observation of this decay chain by finding 6 events, from which we measure: $B(\varphi \to \eta\gamma)/B(\varphi \to \eta'\gamma)$= $(7.3\pm^{4.0}_{2.7}\pm1.1)\times10^{-3}$. Scaling those values by the $\varphi \to \eta\gamma$ branching ratio we obtain: $B(\varphi \to \eta'\gamma) = (8.9 \pm 2.0 \pm 0.5) \times 10^{-5}$.

4.3 $\varphi \longrightarrow f_0\gamma$

The measurement of the branching ratio for this decay can give information on the controversial nature of the f_0 meson. The theoretical prediction for this branching ratio range from 10^{-6} up to 10^{-4} depending on the internal structure of this meson (glueball, $K^0\bar{K^0}$ molecule, four quarks bound state) [7]. The decay chain that we studied is $\varphi \longrightarrow f_0\gamma$, $f_0 \longrightarrow \pi^0\pi^0$. This results in a 5 prompt photons final states where the radiative photon has an energy less than 100 MeV. The main background to this final state is $e^+e^- \longrightarrow \omega\pi^0$ where the ω decaying in $\pi^0\gamma$. This background is effectively reduced by a cut on the angle between a π^0 and the γ in the dipion rest frame. We selected 193 $\pm$ 21 events in the f_0 region (which is defined as M($\pi^0\pi^0$ >700 MeV/c^2)) using 1.84 pb^{-1}. The measured branching ratio is : $B(\varphi \to \pi^0\pi^0\gamma$ (f_0 region))= $(0.8 \pm 0.10 \pm 0.08) \times 10^{-4}$ to be compared to $B = (1.14 \pm 0.10 \pm 0.12) \times 10^{-4}$ (SND-2) and $B = (1.06 \pm 0.09 \pm 0.06) \times 10^{-4}$ (CMD-2).

5 Conclusions

The KLOE detector has been operational on the DAΦNE e$^+$ e$^-$ collider since the beginning of 1999. During this period 2.4 pb^{-1} have been collected. The detector has been calibrated and shows performance close to the design values or better. The first studies on the neutral kaon decays have been performed, measuring basic observables like the K_L and K_S masses and lifetimes and the φ 4-momentum, and the first sample of CP violating $\mathrm{K}_L \longrightarrow \pi^+\pi^-$ events have been seen. With the integrated luminosity collected we already performed significant measurements of some φ radiative decays of interest and in particular we obtained preliminary results on the measurement of the following branching ratios:

$B(\varphi \to \eta\gamma)/B(\varphi \to \pi^0\gamma) = 3.75 \pm 0.08 \pm 0.24$,
$B(\varphi \to \eta'\gamma) = (8.9 \pm 2.0 \pm 0.5) \times 10^{-5}$,
$B(\varphi \to \pi^0\pi^0\gamma$ (f_0 region))= $(0.8 \pm 0.10 \pm 0.08) \times 10^{-4}$.

1. The KLOE collaboration., KLOE, a general purpose detector for DAΦNE, LNF-92/019 (IR) (1992).
2. G. Vignola, Proc. of EPAC96, Sitges, Spain, June 10-14 1996
3. Particle Data Group, Eur Phys. J. C3 (1998)
4. NA31 Collaboration, Phys. Lett. B317, 233 (1992); E731 Collaboration, Phys. Rev. Lett. 70, 1199 (1993)
5. The KLOE collaboration, The KLOE detector, Technical Proposal, LNF-93/002 (IR) (1993).
6. The KLOE collaboration, The KLOE Central Drift Chamber, addendum to the KLOE technical proposal, LNF-94/028 (IR) (1994).
7. R.J. Jaffe, Phys. Rev D15 (1977), 267 ; J. Weinstein N. Isgur, Phys. Rev. D41 (1990), 2236; R.J. Jaffe, K. Jhonson, Phys. Lett. B60 (1976),201.